

Exploration of Pyrazolo[1,5-*a*]pyrimidines as Membrane-Bound Pyrophosphatase Inhibitors

Niklas G. Johansson,^[a] Loïc Dreano,^[a] Keni Vidilaseris,^[b] Ayman Khattab,^[c] Jianing Liu,^[b] Arthur Lasbleiz,^[a] Orquidea Ribeiro,^[b] Alexandros Kiriazis,^[a] Gustav Boije af Gennäs,^[a] Seppo Meri,^[c] Adrian Goldman,^[b, d] Jari Yli-Kauhaluoma,^[a] and Henri Xhaard*^[a]

Inhibition of membrane-bound pyrophosphatase (mPPase) with small molecules offer a new approach in the fight against pathogenic protozoan parasites. mPPases are absent in humans, but essential for many protists as they couple pyrophosphate hydrolysis to the active transport of protons or sodium ions across acidocalcisomal membranes. So far, only few nonphosphorus inhibitors have been reported. Here, we explore the chemical space around previous hits using a combination of screening and synthetic medicinal chemistry, identifying com-

pounds with low micromolar inhibitory activities in the *Thermotoga maritima* mPPase test system. We furthermore provide early structure-activity relationships around a new scaffold having a pyrazolo[1,5-*a*]pyrimidine core. The most promising pyrazolo[1,5-*a*]pyrimidine congener was further investigated and found to inhibit *Plasmodium falciparum* mPPase in membranes as well as the growth of *P. falciparum* in an *ex vivo* survival assay.

Introduction

Parasitic human diseases, such as malaria, leishmaniasis, trypanosomiasis and toxoplasmosis, represent a severe global health concern. The life cycles of protozoan parasites, including *Plasmodium* spp., *Leishmania* spp., *Trypanosoma* spp. and *Toxoplasma* spp., are rather complex and typically comprise of transitions between hosts and vectors as well as intracellular and extracellular environments. To survive these changes, the protozoan cell must be able to adjust e.g. for fluctuating osmotic pressures. The key mechanism involves membrane-bound pyrophosphatases (mPPases).^[1] These enzymes are located in the cell membrane of bacteria and archaea, but can also be found in the protist acidocalcisome, and in the Golgi

apparatus and/or the vacuole of plants and algae.^[2–8] mPPases are important for many protists by acting as ion pumps through pyrophosphate hydrolysis.^[9–12] As shown by knock-out and knock-down studies in *P. falciparum*,^[13] *T. brucei*^[14] and *T. gondii*,^[15] mPPases are required for maintaining *in vitro* asexual blood stage growth, acidocalcisome acidification and parasitic virulence. Moreover, *T. gondii* intracellular proliferation was retarded by mPPase-inhibiting bisphosphonate derivatives.^[16] In recent years, various crystal structures of mung bean *Vigna radiata*^[17,18] and hyperthermophilic bacterium *Thermotoga maritima*^[17,19,20] mPPases have been solved by us and others.

mPPases are promising therapeutic targets as they play an important role in the lifecycle of many protists but do not exist in multicellular animals.^[9–12] In addition, their three-dimensional structures have been solved in diverse conformations, which makes them amenable to structure-based design. Only a few small molecule inhibitors have been however reported so far. A main class is formed by nonhydrolyzable pyrophosphate (PP_i) analogues, which have the drawback of interfering with several human enzymes hydrolyzing or producing PP_i. Examples include ectonucleotide pyrophosphatases, phosphodiesterases and inorganic pyrophosphatases.^[21]


Previously, we developed a 96-well plate *in vitro* screening assay using thermostable *Thermotoga maritima* mPPase (TmPPase) as a model enzyme, and discovered several classes of nonphosphorus inhibitors.^[22,23] By screening of commercially available compounds as well as synthetic medicinal chemistry, we explored and identified several low micromolar hits (compounds 1–5; Figure 1).^[24] Among those, the isoxazole-based compound 2 retained activity *ex vivo* against *P. falciparum*.^[24] The binding location of the isoxazoles, whether at the catalytic site or elsewhere, could not be determined experimentally. In contrast, we have demonstrated using X-ray crystallography that the 2-aminobenzothiazole 1 binds allosteri-

[a] N. G. Johansson, L. Dreano, A. Lasbleiz, Dr. A. Kiriazis, Dr. G. Boije af Gennäs, Prof. J. Yli-Kauhaluoma, Dr. H. Xhaard Drug Research Program, Division of Pharmaceutical Chemistry and Technology, Faculty of Pharmacy University of Helsinki, P.O. Box 56 (Viikinkaari 5 E), 00014 Helsinki (Finland) E-mail: henri.xhaard@helsinki.fi


[b] Dr. K. Vidilaseris, J. Liu, Dr. O. Ribeiro, Prof. A. Goldman Department of Biosciences, Division of Biochemistry University of Helsinki, P.O. Box 56 (Viikinkaari 9), 00014 Helsinki (Finland)

[c] Dr. A. Khattab, Prof. S. Meri Malaria Research Laboratory, Translational Immunology Research Program, Department of Bacteriology and Immunology, Haartman Institute University of Helsinki, P.O. Box 21 (Haartmaninkatu 3), 00014 Helsinki (Finland)

[d] Prof. A. Goldman School of Biomedical Sciences and Astbury Centre for Structural Molecular Biology University of Leeds, Clarendon Way, Leeds LS2 9JT (UK)

 Supporting information for this article is available on the WWW under <https://doi.org/10.1002/cmdc.202100392>

 This article belongs to the Special Collection "Nordic Medicinal Chemistry".

 © 2021 The Authors. ChemMedChem published by Wiley-VCH GmbH. This is an open access article under the terms of the Creative Commons Attribution License, which permits use, distribution and reproduction in any medium, provided the original work is properly cited.

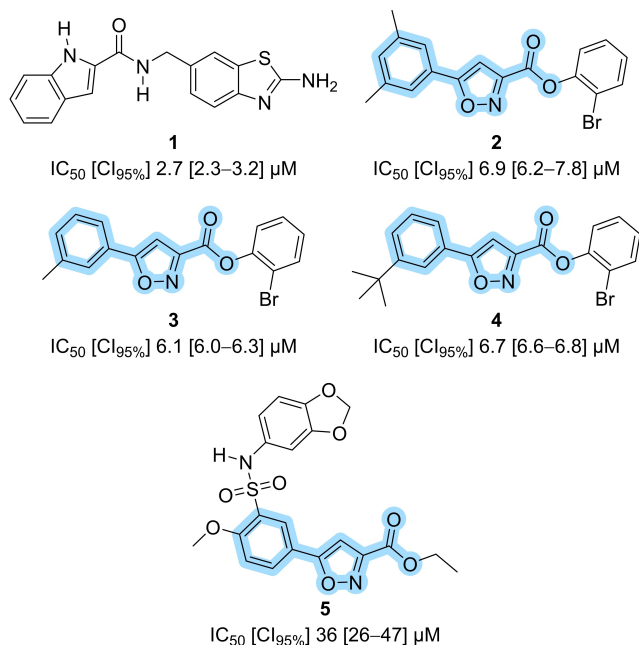


Figure 1. Selected examples of nonphosphorus mPPase inhibitors previously reported.^[20,24] Blue highlight, common substructure used for similarity searches in this manuscript; IC₅₀, half maximal inhibitory concentration; CI_{95%}, half maximal inhibitory concentration expressed as a 95% confidence interval (given in square brackets).

cally outside the catalytic side, near the so-called exit channel (PDB code: 6QXA).^[20]

Here, starting from **2** and its congeners, we aimed to identify novel molecular scaffolds that would lead to gain in binding affinity. These could be translated into therapeutic molecules but could also have a higher probability to be co-crystallized at the mPPase catalytic site, which so far has eluded us. Following a screening of 52 compounds, we set to explore the pyrazolo[1,5-*a*]pyrimidine core. An advantage of swapping the central core structure is that it would allow further chemical expansion of the 2-position in pyrazolo[1,5-*a*]pyrimidines via Suzuki coupling or other coupling methods. Furthermore, pyrazolo[1,5-*a*]pyrimidines^[25] have been reported to have antibacterial activity against *Mycobacterium tuberculosis*,^[26] antiparasitic activity including antileishmanial,^[27] antimalarial (*P. falciparum* dihydroorotate dehydrogenase inhibitors)^[28] and antitrypanosomal,^[27] as well as antiviral activity against HIV.^[29]

Results and Discussion

Exploration of the isoxazole and sulfonamide space through screening

We started from the previously identified 5-arylisoxazole-3-carboxylate core present in **2–5** (Figure 1, highlighted in blue). Using KNIME,^[30] we did a substructure search for commercial analogues in the ZINC12 database^[31] From our experience, computational methods (including docking simulations) do not

offer a robust and/or reliable mean of prioritization at the mPPase. Therefore, we manually picked compounds from a diverse collection provided by a single vendor (Ambinter, 174 matches for the substructure query). Out of the search results, we selected fifteen isoxazoles for testing *in vitro*. For all compounds in this manuscript, we tested activity using a 96-well based assay that detects the inhibition of TmPPase.^[22–24]

In this first set (Supporting Information, Table S1 and S2), eleven of the fifteen isoxazoles had a sulfonamide-linked 2-methoxyphenyl moiety. The sulfonamides **6** and **7** (Figure 2) were the two best compounds with **6** (IC₅₀ = 5.4 μM) being one of the most potent TmPPase inhibitors found thus far. Interestingly, in comparison with **7–10**, the sulfonamide-linked 2,3,4,5-tetrahydrobenzo[*b*][1,4]thiazepine moiety found in **6** is critical for mPPase activity. Even the simple addition of a methyl group (as in **8**) was not tolerated. Also, minor alterations of the seven-membered ring (as in **9** and **10**) caused the loss of all TmPPase inhibitory activity. Other ring modifications also proved unsuccessful (Table S2). Because of the sharp, difficult to rationalize, structure-activity relationships of the isoxazole-sulfonamide core, we in this manuscript decided to pursue other scaffolds (see below).

We also tested another set of 18 sulfonamides (Table S3) and 19 amides (Table S4) that were readily available to us and thus were candidates for repurposing. These compounds share some chemical features with **2**, with many having a central polar core bearing N and/or O atoms surrounded by more

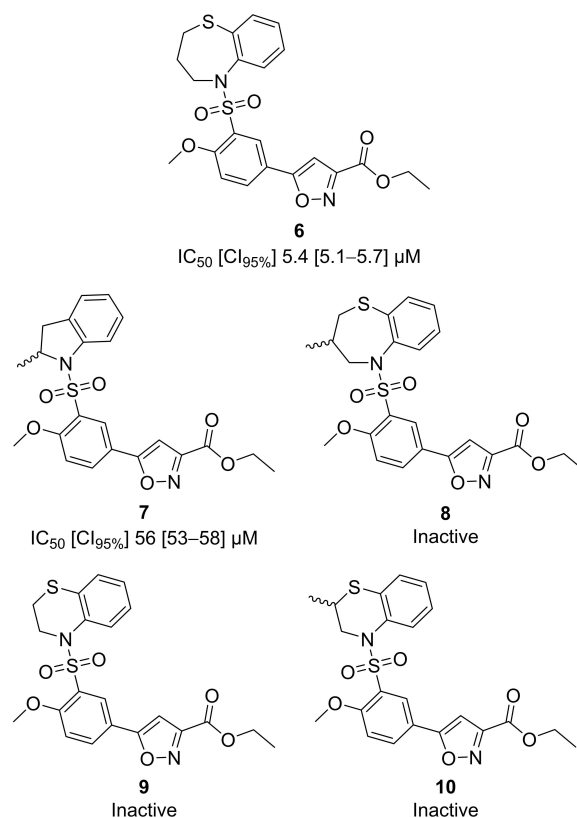


Figure 2. Top two compounds and some of their inactive analogues from the substructure-based search.

hydrophobic/aromatic functional groups. Of this set, compounds **11** and **12** (Figure 3) were the most potent with IC_{50} values below 25 μ M. Sulfonamide **11** (IC_{50} = 14 μ M; ligand efficiency (LE) = 0.23) share the 2-methoxyphenyl-sulfonamide moiety of **6** but lacks its isoxazole core, and therefore shows potential for further exploration. Compound **12** (IC_{50} = 25 μ M) is structurally different from the hitherto most potent nonphosphorus TmPPase inhibitors and thus was picked as a template for further design. Compound **12** was the only compound from this subset with a 4,5-dihydropyrrolo[3,4-*c*]pyrazol-6(1*H*)-one core.

Chemical exploration of the pyrazolo[1,5-*a*]pyrimidine core

Next, we decided to further explore the chemical space around the recently discovered 4,5-dihydropyrrolo[3,4-*c*]pyrazol-6(1*H*)-one scaffold, using combinations of substituents already found to be favorable for activity. We nonetheless decided to swap the original bicyclic scaffold with a related nitrogen-rich, pyrazolo[1,5-*a*]pyrimidine core. This approach was synthetically more achievable, allowing easy modifications at three positions. In addition, the synthetic exploration could take advantage of readily available starting materials, such as various aromatic or aliphatic ketones. The scaffold change can be rationalized by

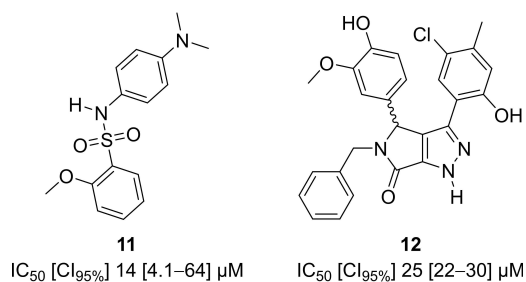
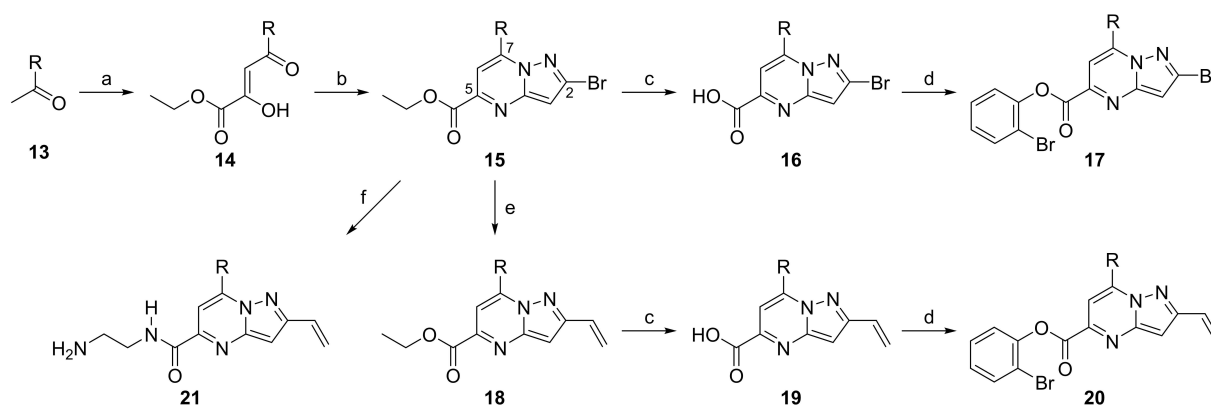


Figure 3. Best hits from the readily available compound set.



Scheme 1. Synthesis of compounds **14**–**21**. Reagents and conditions: (a) *t*-BuOK, diethyl oxalate, THF, rt, 1 h, 87–88%; (b) 5-Bromo-1*H*-pyrazol-3-amine; HCl (aq), EtOH, mw, 78 °C, 30 min, 64–81%; (c) LiOH, EtOH/H₂O, rt, overnight, 89–96%; (d) 2-Bromophenol, HATU, DIPEA, DMF, rt, overnight, 36–61%; (e) Potassium vinyltrifluoroborate, Et₃N, Pd(dppf)Cl₂, EtOH, mw, 125 °C, 15 min, 53–56%; (f) Potassium vinyltrifluoroborate, ethylenediamine, Pd(dppf)Cl₂, *n*-PrOH, mw, 125 °C, 15–30 min, 49–87%.

comparing the pharmacophores of **17a** with **2** and **12** (Supporting Information, Figure S1 and S2).

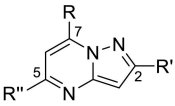
We relied on a method reported by Childress et al.^[32] as we could adapt the first two steps of their synthesis route to access the key intermediate **15** (Scheme 1). Crossed condensation at room temperature of commercially available 3,5-dimethylacetophenone or acetylcyclopropane with diethyl oxalate and potassium *tert*-butoxide in THF gave **14**. Subsequent ring condensation of **14** with 3-bromo-1*H*-pyrazol-5-amine in refluxing ethanol resulted in the formation of pyrazolo[1,5-*a*]pyrimidine **15**. Hydrolysis of the formed ethyl ester **15** using lithium hydroxide in a mixture of ethanol and water gave the corresponding carboxylic acid **16**, which was reacted with 2-bromophenol and 1-[bis(dimethylamino)methylene]-1*H*-1,2,3-triazolo[4,5-*b*]pyridinium 3-oxide hexafluorophosphate (HATU) and 2-bromophenol to give the desired 2-bromophenyl carboxylate **17**.

The bromine substituent in the 2-position of **15** could serve as a coupling handle for further exploration of the chemical space by various Pd-mediated cross-coupling reactions. Suzuki coupling of ethyl ester **15** in *n*-propanol with commercially available potassium vinyltrifluoroborate was done under microwave conditions. The product obtained, **18**, could be transformed into the corresponding 2-bromophenyl ester **20** following the same hydrolysis and esterification procedures used for **16** and **17**, respectively. However, changing trimethylamine used in the Suzuki coupling to ethylenediamine serendipitously led to both Suzuki coupling and amidation occurring in the same reaction mixture, yielding **21** in a single step.

Biological activity of the pyrazolo[1,5-*a*]pyrimidine core

We started our exploration by taking inspiration from **12** (IC_{50} = 25 μ M) and changing the isoxazole core of **2** (IC_{50} = 6.9 μ M) to the corresponding pyrazolo[1,5-*a*]pyrimidine analogue **17a** (Table 1). This scaffold change was relatively well tolerated, with just a 2-fold loss in activity compared to **2**. As previously

Table 1. Activities of the pyrazolo[1,5-*a*]pyrimidine series.

									
compound	R	R'	R''	IC ₅₀ [CI _{95%}]	compound	R	R'	R''	IC ₅₀ [CI _{95%}]
15a				120 [110–140] μM	15b				150 [130–180] μM
16a				NA [NA–NA] μM	16b				NA [NA–NA] μM
17a				14 [13–15] μM	17b				NA [NA–NA] μM
18a				54 [51–58] μM	18b				NA [NA–NA] μM
19a				14 [13–15] μM	19b				NA [NA–NA] μM
20a				18 [17–19] μM	20b				NA [NA–NA] μM
21a				72 [61–85] μM	21b				260 [190–360] μM

noticed for the isoxazole series,^[24] the corresponding carboxylic acid **16a** was inactive, but the ethyl ester **15a** retained weak activity.

Since the central pyrazolo[1,5-*a*]pyrimidine core is bulkier than the original isoxazole moiety (the molecular weight of **17a** is approximately 500 Da), we tried to introduce lighter substitutions. The exchange of the R-group at the 7-position, from a 3,5-dimethylphenyl group to a cyclopropyl ring, was only slightly effective for the ethyl carboxylate **15b**. Furthermore, it proved completely unsuccessful for the carboxylic acid **16b** and the 2-bromophenyl carboxylate **17b**. Similarly, replacing the R-substituent with other phenyl moieties than the original 3,5-dimethylphenyl substituent (unsubstituted or bearing electron withdrawing/donating groups), were generally not well tolerated for the isoxazole derivatives.^[24]

We next studied further functionalization of the 2-position in pyrazolo[1,5-*a*]pyrimidines. Bromine atoms are very useful in X-ray crystallography (due to their anomalous scattering, which can aid in identifying the presence of the compound as well as its orientation in low-resolution, 3.5 Å or worse). Additionally, aryl bromides are highly useful e.g. in Suzuki coupling with various organoboron substrates. We introduced a well-accepted vinyl group at the 5-position, showing nearly no loss of activity for **20a** in comparison to the hitherto best pyrazolo[1,5-*a*]pyrimidine **17a** (IC₅₀ = 14 μM). Moreover, there was a 2.2-fold improvement in the inhibition comparing the ethyl ester **18a** to the 2-bromo analogues **15a**. Interestingly, the 2-vinyl-substituted carboxylic acid **19a** (IC₅₀ = 14 μM) was as active as the

best pyrazolo[1,5-*a*]pyrimidines and superior to its inactive 2-bromo analogue **16a**. As presented above, the corresponding 2-vinyl-substituted cyclopropyl analogues **18b–20b** were all inactive. In the same way, the 3,5-dimethylphenyl-substituted amide **21a** showed 3.6-fold higher inhibition than the corresponding cyclopropyl-substituted analogue **21b**.

Follow-up studies of **12**, **17a**, **19a** and **20a**

In order to rule out a cause of false positives, colloidal aggregation in the TmPPase model assay was evaluated for compounds **17a**, **19a** and **20a** at six concentrations (100 μM, 50 μM, 20 μM, 10 μM, 1 μM, and 0.1 μM) using the assay conditions (Figure S3). Compounds **17a** and **20a** showed aggregate formation at concentrations above 20 μM, which is above their IC₅₀ values. Compound **19a** showed no detectable aggregation.

Further hit validation was done against the purified mPPase from *P. falciparum* (PfPPase-VP1) expressed in baculovirus-infected insect cells. Compound **17a** was able to inhibit the PfPPase-VP1 activity with an IC₅₀ of 58 μM (Figure 4A). Compounds **19a** and **20a** had lower inhibition activities with IC₅₀ values of 130 μM and 74 μM, respectively (Figure S5). Overall, these compounds have higher IC₅₀ values for PfPPase-VP1 than for TmPPase. In a survival assay in erythrocytes culture **17a** was able to inhibit the growth of *P. falciparum* with an IC₅₀ of 31 μM (Figure 4B), better than its inhibition on the PfPPase-VP1. This

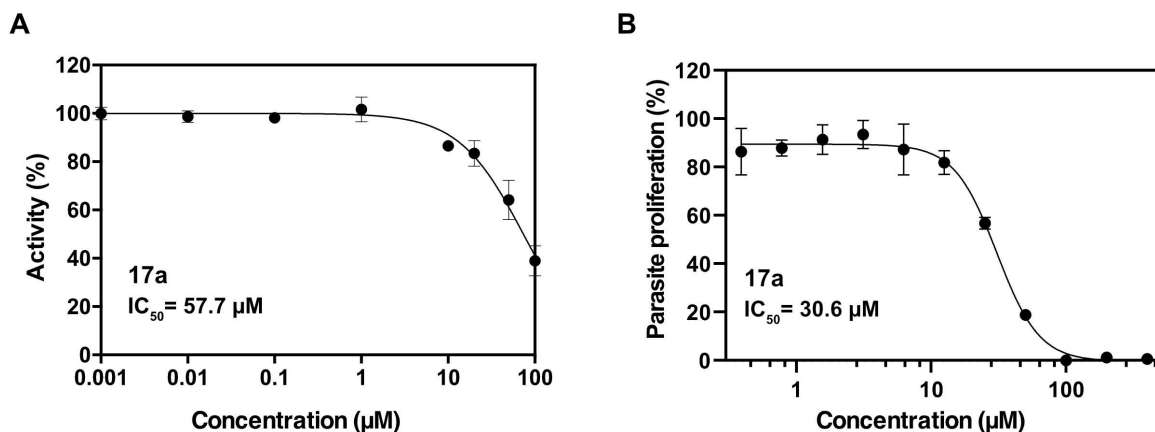


Figure 4. (A) Inhibition of *P. falciparum* mPPase (PfPPaseVP-1) by 17a. (B) Effect of 17a on *P. falciparum* growth. All data are shown as mean \pm SD in three replicates.

could mean that the compound inhibits other proteins in the parasite, e.g. through soluble pyrophosphatase, or via some other mechanism, which could be linked to colloidal aggregation. Interestingly, compound 12 was able to inhibit the growth of *P. falciparum* with the IC_{50} of 3.6 μ M (Figure S6) even though the activity on PfPPase-VP1 (Figure S4) was comparably weak. No hemolysis of human erythrocytes was observed, suggesting no significant cytotoxicity.^[33]

Conclusion

Altogether, this manuscript presents novel scaffolds with potential for further exploration in the drug discovery against parasitic diseases. Using a screening approach (52 compounds) together with a medicinal chemistry exploration (14 compounds) and the TmPPase test system, we discovered new TmPPase inhibitors: the 4,5-dihydropyrrolo[3,4-*c*]pyrazol-6(1*H*)-one core (compound 12) and pyrazolo[1,5-*a*]pyrimidines (17a, 19a and 20a). We explored the SARs around this latter core and maintained low micromolar activity (IC_{50} = 14–18 μ M) for three of the synthesized pyrazolo[1,5-*a*]pyrimidines. Molecular modelling suggests that the substrate binding sites are highly conserved in many protozoan pathogens, which should allow transferability of the findings.^[11,34] Indeed, compound 17a binds to the PfPPase-VP1 with an IC_{50} of 58 μ M and inhibits parasite growth.

Experimental Section

Computational methods

Pharmacophore modelling was conducted using the Schrödinger Maestro suite.^[35] Substructure searches were conducted from the

ZINC12 database^[31] (clean drug-like subset; 13,195,609 compounds; downloaded on 2018.11.11). Ligand efficiencies were computed using the pIC_{50} and the “Heavy Atom Count” normalization method with Accelrys’s Discovery Studio.^[36]

Chemistry

General experimental methods: All chemicals were available from commercial vendors and used without any further purification. Anhydrous reactions were conducted in oven-dried (130 °C, > 24 h) glassware that were purged with argon prior to use. Microwave reactions were done in sealed reaction vials using a Biotage[®] Initiator⁺ instrument (Uppsala, Sweden). The progress of the reactions was monitored using thin-layer chromatography on silica gel 60-F₂₅₄ aluminum plates and visualized by a dual short/long wave (254/366 nm) UV lamp. Combined organic solutions from extractions were dried over anhydrous Na₂SO₄, filtered and concentrated with a rotary evaporator at reduced pressure. Flash SiO₂ column chromatography was performed with automated high performance flash chromatography, Biotage[®] Isolera™ Spektra Systems with ACI™ and Assist (ISO-15W Isolera One) equipped with a variable UV-VIS (200–800 nm) photodiode array (Uppsala, Sweden) using SNAP KP-Sil/Ultra 10, 25, 50 or 100 g cartridges and the indicated mobile phase gradient. The reactions were not optimized and all the yields are given for purified products.

The synthesized products were characterized by NMR and MS analysis. ¹H and ¹³C NMR spectra were acquired at 298 K on a Bruker Ascend 400 MHz-Avance III HD NMR spectrometer (Bruker Corporation, Billerica, MA, USA). Chemical shifts (δ) are reported in parts per million (ppm) relative to the residual solvent signals: CDCl₃ 7.26 and 77.16 ppm, CD₃OD 3.31 and 49.00 ppm for ¹H and ¹³C NMR, respectively. Multiplicities are indicated as bs (broad singlet), s (singlet), d (doublet), t (triplet), q (quartet), dd (doublet of doublets), tt (triplet of triplets) and m (multiplet). Purity of the final compounds (> 95%) was confirmed by LC-MS using a Waters Acquity[®] UPLC system (Waters, Milford, MA, USA) equipped with an Acquity PDA detector, a Waters Synapt G2 HDMS mass spectrometer (Waters, Milford, MA, USA) and an Acquity UPLC[®] BEH C18 column (1.7 μ m, 50 mm \times 2.1 mm, Waters, Ireland). Mass range was set from 100 to 600 Da. High resolution mass (HRMS-ESI) data was

reported for the calculated and experimentally found molecular ions $[M+H]^+$ or $[M-H]^-$.

General procedure for synthesis of compound 14: The synthesis of compound **14** was adapted from a previously described method.^[32] In brief, *t*-BuOK (2 equiv) was dissolved in anhydrous THF (1.2 mL/mmol) under argon, followed by addition of diethyl oxalate (2 equiv) and the mixture was stirred for 30 min. Then, ketone **13** (1 equiv) dissolved in anhydrous THF (2.2 mL/mmol) was added dropwise and stirred for 1 h. The reaction was quenched by addition of a 1 M solution of HCl in H₂O (3.0 mL/mmol).

Ethyl 4-(3,5-dimethylphenyl)-2-hydroxy-4-oxobut-2-enoate (14a): 1-(3,5-Dimethylphenyl)ethan-1-one (2.0 g, 13 mmol) was used to give **14a** (2.9 g, 88%) as a yellow solid. ¹H NMR (400 MHz, CDCl₃): δ = 7.59 (s, 2H), 7.23 (s, 1H), 7.04 (s, 1H), 4.40 (q, *J* = 7.1 Hz, 2H), 2.38 (s, 6H), 1.41 (t, *J* = 7.1 Hz, 3H), 1H not observed (exchangeable); ¹³C NMR (101 MHz, CDCl₃): δ = 191.3, 169.6, 162.4, 138.7, 135.7, 135.0, 125.8, 98.2, 62.7, 21.3, 14.2.

Ethyl 4-cyclopropyl-2-hydroxy-4-oxobut-2-enoate (14b): 1-Cyclopropylethan-1-one (1.4 g, 17 mmol) was used to give **14b** (2.8 g, 87%) as a pale yellow liquid. ¹H NMR (400 MHz, CDCl₃): δ = 6.46 (s, 1H), 4.33 (q, *J* = 7.1 Hz, 2H), 1.87 (tt, *J* = 7.8, 4.5 Hz, 1H), 1.35 (t, *J* = 7.1 Hz, 3H), 1.22–1.17 (m, 2H), 1.08–1.02 (m, 2H), 1H not observed (exchangeable); ¹³C NMR (101 MHz, CDCl₃): δ = 204.7, 163.2, 162.4, 102.2, 62.5, 20.8, 14.1, 12.3.

General procedure for synthesis of compound 15: The synthesis of compound **15** was adapted from a previously reported method.^[32] Briefly, to a solution of **14** (1 equiv) in EtOH (5.0 mL/mmol) were added a catalytic amount of a 1 M solution of HCl in H₂O (5 drops) and 5-bromo-1*H*-pyrazol-3-amine (1.25 equiv). The reaction mixture heated by microwave irradiation at 78 °C for 30 min, followed by filtration once the product had precipitated.

Ethyl 2-bromo-7-(3,5-dimethylphenyl)pyrazolo[1,5-*a*]pyrimidine-5-carboxylate (15a): Compound **14a** (1.0 g, 4.1 mmol) was used to give **15a** (1.2 g, 81%) as a pale yellow solid. ¹H NMR (400 MHz, CDCl₃): δ = 7.65 (s, 2H), 7.64 (s, 1H), 7.22 (s, 1H), 7.02 (s, 1H), 4.54 (q, *J* = 7.1 Hz, 2H), 2.42 (s, 6H), 1.48 (t, *J* = 7.1 Hz, 3H); ¹³C NMR (101 MHz, CDCl₃): δ = 164.0, 149.8, 147.6, 147.3, 138.7, 136.1, 133.7, 129.9, 127.1, 107.4, 102.1, 62.9, 21.5, 14.4; HRMS (ESI) *m/z*: $[M+H]^+$ calcd for C₁₇H₁₇BrN₃O₂ 374.0504, found 374.0503.

Ethyl 2-bromo-7-cyclopropylpyrazolo[1,5-*a*]pyrimidine-5-carboxylate (15b): Compound **14b** (0.77 g, 4.2 mmol) was used to give **15b** (0.82 g, 64%) as a white solid. ¹H NMR (400 MHz, CDCl₃): δ = 7.05 (s, 1H), 6.93 (s, 1H), 4.49 (q, *J* = 7.1 Hz, 2H), 2.91 (tt, *J* = 8.5, 5.3 Hz, 1H), 1.47–1.38 (m, 5H), 1.19–1.13 (m, 2H); ¹³C NMR (101 MHz, CDCl₃): 164.1, 153.3, 148.7, 147.2, 135.8, 101.8, 101.1, 62.9, 14.4, 10.8, 10.7; HRMS (ESI) *m/z*: $[M+H]^+$ calcd for C₁₂H₁₃BrN₃O₂ 310.0191, found 310.0190.

General procedure for synthesis of compounds 16 and 19: The synthesis of compounds **16** and **19** were done according to a method described elsewhere.^[24] In brief, a mixture of the ethyl ester (1 equiv) and LiOH (2 equiv) in a 4:1 ratio of EtOH/H₂O (75 mL/mmol) was stirred for 16 h (3 d for **16b**), followed by back-extraction.

2-Bromo-7-(3,5-dimethylphenyl)pyrazolo[1,5-*a*]pyrimidine-5-carboxylic acid (16a): Compound **15a** (0.30 g, 0.80 mmol) was used to give **16a** (0.25 g, 89%) as a pale yellow solid. ¹H NMR (400 MHz, CD₃OD): δ = 7.69 (s, 2H), 7.67 (s, 1H), 7.28 (s, 1H), 7.01 (s, 1H), 2.43 (s, 6H); ¹³C NMR (101 MHz, CD₃OD): δ = 166.5, 151.0, 149.7, 149.0, 139.8, 136.7, 134.3, 131.3, 128.2, 108.4, 102.0, 21.4; HRMS (ESI) *m/z*: $[M+H]^+$ calcd for C₁₅H₁₃BrN₃O₂ 346.0191, found 346.0196.

2-Bromo-7-cyclopropylpyrazolo[1,5-*a*]pyrimidine-5-carboxylic acid (16b): Compound **15b** (0.15 g, 0.49 mmol) was used to give **16b** (0.12 g, 90%) as a white solid. ¹H NMR (400 MHz, CD₃OD): δ = 7.13 (s, 1H), 6.91 (s, 1H), 2.98 (tt, *J* = 8.4, 5.1 Hz, 1H), 1.51–1.44 (m, 2H), 1.25–1.19 (m, 2H); ¹³C NMR (101 MHz, CD₃OD): δ = 163.5, 155.1, 147.5, 145.5, 136.5, 101.3, 99.5, 11.4; 11.1; HRMS (ESI) *m/z*: $[M+H]^+$ calcd for C₁₀H₉BrN₃O₂ 281.9878, found 281.9876.

7-(3,5-Dimethylphenyl)-2-vinylpyrazolo[1,5-*a*]pyrimidine-5-carboxylic acid (19a): Compound **18a** (0.23 g, 0.71 mmol) was used to give **19a** (0.20 g, 96%) as a yellow solid. ¹H NMR (400 MHz, CD₃OD): δ = 7.63 (s, 2H), 7.53 (s, 1H), 7.19 (s, 1H), 7.00 (s, 1H), 6.85 (dd, *J* = 17.7, 11.0 Hz, 1H), 6.12 (dd, *J* = 17.7, 1.3 Hz, 1H), 5.56 (dd, *J* = 11.0, 1.3 Hz, 1H), 2.37 (s, 6H); ¹³C NMR (101 MHz, CD₃OD): δ = 166.5, 157.8, 150.8, 148.7, 148.2, 139.6, 134.0, 131.7, 130.2, 128.1, 120.3, 107.7, 96.0, 21.4; HRMS (ESI) *m/z*: $[M+H]^+$ calcd for C₁₇H₁₆N₃O₂ 294.1242, found 294.1246.

7-Cyclopropyl-2-vinylpyrazolo[1,5-*a*]pyrimidine-5-carboxylic acid (19b): Compound **18b** (0.10 g, 0.40 mmol) was used to give **19b** (0.88 mg, 96%) as a pale yellow solid. ¹H NMR (400 MHz, CD₃OD): δ = 6.98 (s, 1H), 6.83 (s, 1H), 6.81 (dd, *J* = 17.8, 11.1 Hz, 1H), 6.07 (dd, *J* = 17.8, 1.2 Hz, 1H), 5.52 (dd, *J* = 11.1, 1.2 Hz, 1H), 2.78 (tt, *J* = 8.4, 5.1 Hz, 1H), 1.37–1.29 (m, 2H), 1.17–1.10 (m, 2H); ¹³C NMR (101 MHz, CD₃OD): δ = 166.4, 157.4, 154.5, 149.4, 147.9, 130.1, 120.1, 101.7, 95.7, 11.5, 10.4; HRMS (ESI) *m/z*: $[M+H]^+$ calcd for C₁₂H₁₂N₃O₂ 230.0930, found 230.0932.

General procedure for synthesis of compounds 17 and 20: The carboxylic acid (1 equiv) was dissolved in anhydrous DMF (3.3 mL/mmol) under argon, followed by *N,N*-diisopropylethylamine (DIPEA; 2.5 equiv) and stirred for 15 min at room temperature. HATU (1.2 equiv) and 2-bromophenol (1.3 equiv) were subsequently added and the mixture was stirred for 16 h. The mixture was diluted with EtOAc and washed once with a 0.05 M solution of HCl in H₂O (2.5 equiv), three times with a half-saturated solution of NaHCO₃ in H₂O, brine, dried with Na₂SO₄, filtered, evaporated and the residue was purified by flash chromatography with *n*-hexane/EtOAc (1:0→0:1) as eluent.

2-Bromophenyl 2-bromo-7-(3,5-dimethylphenyl)pyrazolo[1,5-*a*]pyrimidine-5-carboxylate (17a): Compound **16a** (0.051 g, 0.15 mmol) was used to give **17a** (0.027 g, 36%) as a pale yellow solid. ¹H NMR (400 MHz, CDCl₃): δ = 7.80 (s, 1H), 7.71–7.66 (m, 3H), 7.44–7.39 (m, 1H), 7.33 (dd, *J* = 8.1, 1.6 Hz, 1H), 7.25–7.19 (m, 2H), 7.12 (s, 1H), 2.45 (s, 6H); ¹³C NMR (101 MHz, CDCl₃): δ = 161.7, 149.9, 148.4, 147.9, 145.8, 138.8, 136.5, 133.9, 133.7, 129.8, 128.9, 128.1, 127.2, 123.7, 116.2, 107.8, 102.6, 21.6; HRMS (ESI) *m/z*: $[M+H]^+$ calcd for C₂₁H₁₆Br₂N₃O₂ 499.9609, found 499.9611.

2-Bromophenyl 2-bromo-7-cyclopropylpyrazolo[1,5-*a*]pyrimidine-5-carboxylate (17b): Compound **16b** (0.050 g, 0.18 mmol) was used to give **17b** (0.043 g, 56%) as a white solid. ¹H NMR (400 MHz, CDCl₃): δ = 7.65 (dd, *J* = 8.1, 1.5 Hz, 1H), 7.41–7.36 (m, 1H), 7.29 (dd, *J* = 8.1, 1.5 Hz, 1H), 7.22–7.16 (m, 2H), 7.03 (s, 1H), 2.96 (tt, *J* = 8.4, 5.2 Hz, 1H), 1.48–1.41 (m, 2H), 1.25–1.19 (m, 2H); ¹³C NMR (101 MHz, CDCl₃): δ = 161.8, 153.7, 148.7, 148.3, 145.7, 136.2, 133.6, 128.8, 128.0, 123.7, 116.1, 102.2, 101.5, 11.0, 10.9; HRMS (ESI) *m/z*: $[M+H]^+$ calcd for C₁₆H₁₂Br₂N₃O₂ 435.9296, found 435.9297.

2-Bromophenyl 7-(3,5-dimethylphenyl)-2-vinylpyrazolo[1,5-*a*]pyrimidine-5-carboxylate (20a): Compound **19a** (0.033 g, 0.11 mmol) was used to give **20a** (0.022 g, 43%) as a yellow solid. ¹H NMR (400 MHz, CDCl₃): δ = 7.76 (s, 1H), 7.75 (s, 1H), 7.69 (dd, *J* = 8.0, 1.6 Hz, 1H), 7.44–7.39 (m, 1H), 7.34 (dd, *J* = 8.0, 1.6 Hz, 1H), 7.25–7.18 (m, 2H), 7.14 (s, 1H), 6.94 (dd, *J* = 17.8, 11.0 Hz, 1H), 6.13 (dd, *J* = 17.8, 1.2 Hz, 1H), 5.60 (dd, *J* = 11.0, 1.2 Hz, 1H), 2.45 (s, 6H); ¹³C NMR (101 MHz, CDCl₃): δ = 162.1, 157.0, 150.0, 148.5, 147.6, 144.9, 138.6, 133.7, 133.5, 130.4, 129.2, 128.8, 128.0, 127.2, 123.8, 120.1,

116.3, 107.3, 96.5, 21.5; HRMS (ESI) m/z : $[M+H]^+$ calcd for $C_{23}H_{19}BrN_3O_2$ 448.0661, found 448.0665.

2-Bromophenyl 7-cyclopropyl-2-vinylpyrazolo[1,5-*a*]pyrimidine-5-carboxylate (20b): Compound **19b** (0.034 g, 0.15 mmol) was used to give **20b** (0.035 mg, 61%) as a yellow solid. 1H NMR (400 MHz, $CDCl_3$): δ = 7.66 (dd, J = 8.0, 1.6 Hz, 1H), 7.42–7.36 (m, 1H), 7.30 (dd, J = 8.0, 1.6 Hz, 1H), 7.21–7.15 (m, 2H), 7.04 (s, 1H), 6.94 (dd, J = 17.7, 11.0 Hz, 1H), 6.15 (dd, J = 17.7, 1.2 Hz, 1H), 5.60 (dd, J = 11.0, 1.2 Hz, 1H), 3.00 (tt, J = 8.4, 5.2 Hz, 1H), 1.46–1.39 (m, 2H), 1.24–1.19 (m, 2H); ^{13}C NMR (101 MHz, $CDCl_3$): δ = 162.2, 156.7, 153.3, 148.8, 148.5, 144.8, 133.6, 129.1, 128.8, 127.9, 123.8, 120.0, 116.2, 101.0, 96.4, 10.9, 10.5; HRMS (ESI) m/z : $[M+H]^+$ calcd for $C_{18}H_{15}BrN_3O_2$ 384.0348, found 384.0348.

General procedure for synthesis of compound 18: The synthesis of compound **18** was adapted from a previously reported method.^[32] Briefly, the 2-bromo pyrazolo[1,5-*a*]pyrimidine **15** (1 equiv), potassium vinyltrifluoroborate (1.2 equiv), Et_3N (2 equiv), and $Pd(dppf)Cl_2$ (0.05 equiv) were dissolved in EtOH (7.5 mL/mmol) in a microwave vial and purged with argon for 10 min. The reaction mixture was heated by microwave irradiation at 125 °C for 15 min. Then, the reaction mixture was filtrated through Celite® and purified with automated flash chromatography with *n*-hexane/EtOAc (1:0→0:1) as eluent.

Ethyl 7-(3,5-dimethylphenyl)-2-vinylpyrazolo[1,5-*a*]pyrimidine-5-carboxylate (18a): Compound **17a** (0.50 g, 1.3 mmol) was used to give **18a** (0.23 g, 53%) as a yellow solid. 1H NMR (400 MHz, $CDCl_3$): δ = 7.70 (s, 2H), 7.60 (s, 1H), 7.21 (s, 1H), 7.05 (s, 1H), 6.90 (dd, J = 17.7, 11.0 Hz, 1H), 6.09 (dd, J = 17.7, 1.2 Hz, 1H), 5.56 (dd, J = 11.0, 1.2 Hz, 1H), 4.54 (q, J = 7.1 Hz, 2H), 2.43 (s, 6H), 1.48 (t, J = 7.1 Hz, 3H); ^{13}C NMR (101 MHz, $CDCl_3$): δ = 164.4, 156.6, 149.9, 147.3, 146.5, 138.5, 133.3, 130.6, 129.3, 127.2, 119.7, 106.9, 96.0, 62.7, 21.5, 14.5; HRMS (ESI) m/z : $[M+H]^+$ calcd for $C_{19}H_{20}N_3O_2$ 322.1555, found 322.1554.

Ethyl 7-cyclopropyl-2-vinylpyrazolo[1,5-*a*]pyrimidine-5-carboxylate (18b): Compound **17b** (0.40 g, 1.3 mmol) was used to give **18b** (0.19 g, 56%) as a pale yellow solid. 1H NMR (400 MHz, $CDCl_3$): δ = 6.99 (s, 1H), 6.94 (s, 1H), 6.89 (dd, J = 17.7, 11.0 Hz, 1H), 6.10 (dd, J = 17.7, 1.2 Hz, 1H), 5.55 (dd, J = 11.0, 1.2 Hz, 1H), 4.48 (q, J = 7.1 Hz, 2H), 2.94 (tt, J = 8.5, 5.2 Hz, 1H), 1.43 (t, J = 7.1 Hz, 3H), 1.41–1.33 (m, 2), 1.19–1.11 (m, 2H); ^{13}C NMR (101 MHz, $CDCl_3$): δ = 164.5, 156.3, 153.0, 148.7, 146.3, 129.2, 119.7, 100.6, 96.0, 62.6, 14.4, 10.7, 10.3; HRMS (ESI) m/z : $[M+H]^+$ calcd for $C_{14}H_{16}N_3O_2$ 258.1242, found 258.1245.

General procedure for synthesis of compound 21: 2-Bromo pyrazolo[1,5-*a*]pyrimidine **15** (1 equiv), potassium vinyltrifluoroborate (1.2 equiv), ethylenediamine (4 equiv), and $Pd(dppf)Cl_2$ (0.05 equiv) were dissolved in *n*-PrOH (5.5 mL/mmol) in a microwave vial and purged with argon for 10 min. The reaction mixture was heated by microwave irradiation at 125 °C for 15 min (for **21a**) and 2 × 15 min (for **21b**). Then, the reaction mixture was filtrated through Celite® and purified with automated flash chromatography with *n*-hexane/EtOAc (1:0→0:1) as eluent.

***N*-(2-Aminoethyl)-7-(3,5-dimethylphenyl)-2-vinylpyrazolo[1,5-*a*]pyrimidine-5-carboxamide (21a):** Compound **15a** (0.051 g, 0.14 mmol) was used to give **21a** (0.023 g, 49%) as a yellow solid. 1H NMR (400 MHz, CD_3OD): δ = 7.69 (s, 2H), 7.61 (s, 1H), 7.25 (s, 1H), 6.99 (s, 1H), 6.87 (dd, J = 17.8, 11.1 Hz, 1H), 6.12 (dd, J = 17.8, 1.3 Hz, 1H), 5.57 (dd, J = 11.1, 1.3 Hz, 1H), 3.68 (t, J = 5.9 Hz, 2H), 3.11 (t, J = 5.9 Hz, 2H), 2.41 (s, 6H); ^{13}C NMR (101 MHz, CD_3OD): 166.4, 157.8, 150.6, 149.8, 148.9, 139.7, 134.0, 132.0, 130.3, 128.1, 120.2, 105.8, 95.5, 41.3, 39.9, 21.4; HRMS (ESI) m/z : $[M+H]^+$ calcd for $C_{19}H_{22}N_5O$ 336.1824, found 336.1828.

***N*-(2-Aminoethyl)-7-cyclopropyl-2-vinylpyrazolo[1,5-*a*]pyrimidine-5-carboxamide (21b):** Compound **15b** (0.051 g, 0.16 mmol) was used to give **21b** (0.039 g, 87%) as a pale brown solid. 1H NMR (400 MHz, CD_3OD): δ = 7.07 (s, 1H), 6.87 (s, 1H), 6.7 (dd, J = 17.8, 11.0 Hz, 1H), 6.12 (dd, J = 17.8, 1.3 Hz, 1H), 5.56 (dd, J = 11.0, 1.3 Hz, 1H), 3.63 (t, J = 6.00 Hz, 2H), 3.08 (t, J = 6.00 Hz, 2H), 2.84 (tt, J = 8.4, 5.2 Hz, 1H), 1.39–1.33 (m, 2H), 1.18–1.13 (m, 2H); ^{13}C NMR (101 MHz, CD_3OD): 166.3, 157.4, 154.6, 149.7, 149.3, 130.3, 120.0, 99.8, 95.2, 41.4, 40.3, 11.5, 10.3; HRMS (ESI) m/z : $[M+H]^+$ calcd for $C_{14}H_{18}N_5O$ 272.1511, found 272.1513.

Biological activities

All commercially obtained compounds had purities >90% as specified by the vendor. Synthesized compounds were >95% pure as determined by LC–MS and characterized by HRMS. The inhibition assay was carried out with purified TmPPase as previously reported.^[22–24] The best hits **17a**, **19a**, and **20a**, were validated using eight compound concentrations in triplicate. Further hit validation was done against the purified mPPase from *P. falciparum* (PfPPase-VP1) expressed in baculovirus-infected insect cells (expression, purification and further enzyme analysis will be described in more detail elsewhere). 4 μ L of the purified PfPPase-VP1 (2.0 mg/mL) was reactivated in 96 μ L of reactivation buffer, i.e. 20 mM 2-(*N*-morpholino)ethanesulfonic acid (MES) pH 6.5, 3.5% (v/v) glycerol, 2 mM dithiothreitol (DTT) and 12 mg/mL L- α -phosphatidylcholine from soybean. For each tube strip, 3 μ L of the reactivated PfPPase-VP1 was added into 12 μ L of reaction buffer (200 mM Tris-Cl pH 8.0, 8.0 mM $MgCl_2$, 333 mM KCl, 67 mM NaCl) and 25 μ L of inhibitor solution. The reaction mixtures were incubated at 50 °C for 5 min and the assay was started with the addition of 10 μ L of 2 mM sodium pyrophosphate and further incubation at 50 °C for 45 min. The reaction termination and colour development were done as earlier described.^[22–24]

Plasmodium falciparum parasite strain 3D7 was used for testing the antiparasitic activity of the test compounds. The parasite was maintained in culture as described previously.^[37] Briefly, parasites were cultured in O+ human erythrocytes at 5% haematocrit in RPMI-1640 medium supplemented with 0.5% Albumax II (Gibco, Carlsbad, CA, USA), 200 μ M hypoxanthine (Sigma, St. Louis, MO, USA) and 20 μ g/mL gentamycin (Gibco). Parasites were synchronized with the sorbitol method as described.^[38] Test compounds were dissolved in DMSO to make a stock solution of 10 mM or 50 mM. Two-fold serial dilutions of the test compounds were made in the culture medium to cover either the range of 100 μ M–100 nM or 400 μ M–390 nM. 50 μ L of each dilution were mixed in 96-well plate with 150 μ L of 2% haematocrit of 0.5% parasitemia (ring stage). Compound dilutions were also mixed with 150 μ L of 2% haematocrit of uninfected erythrocytes to serve as baselines for the activity of the coloured compounds. DMSO concentration in the highest compound concentration was 0.8%. After 72 h incubation at 37 °C, the parasite growth was quantified using fluorescent SYBR Green I®-based assay as described.^[39] The half-maximal inhibitory concentration (IC_{50}) of the test compounds was assessed using the non-linear regression fit model in Prism 7 (GraphPad Software, San Diego, CA, USA). The potent anti-malarial drug, artemisinin, was used in parallel as a positive control. Each concentration of the test compounds was tested in duplicate and the assay was repeated three times. The mean and standard deviation of the three repeats were used to calculate the IC_{50} .

Acknowledgements

This work was funded by grants from the Academy of Finland (No. 265481 to J.Y.-K., No. 308105 to K.V., No. 310297 to H.X., No. 1323237 to S.M. and 1322609 to A.G.), Jane and Aatos Erkko Foundation (to A.G., H.X., and J.Y.-K.; and to S.M. and A.K.), the Biotechnology and Biological Sciences Research Council (BBSRC, No. BB/M021610/1 to A.G.), Sigrid Jusélius Foundation (to S.M.), the Finnish Pharmaceutical Society (to N.G.J.), Magnus Ehrnrooth Foundation (to N.G.J.) and the Swedish Cultural Foundation in Finland (to N.G.J.). Furthermore, the authors wish to gratefully acknowledge CSC-IT Center for Science, and the Drug Discovery and Chemical Biology (DDCB) network for computational resources; Nina Sipari, from the Viikki Metabolomics Unit-Helsinki Institute of Life Science (HiLIFE) for mass spectrometry services; and Dr. Ainoleena Turku for preliminary work on the project.

Conflict of Interest

The authors declare no conflict of interest.

Keywords: membrane-bound pyrophosphatase · antiprotozoal agents · pyrazolo[1,5-a]pyrimidine · inhibitor · drug discovery

- [1] A. O. M. Holmes, A. C. Kalli, A. Goldman, *Front. Mol. Biosci.* **2019**, *6*, 132.
- [2] A. A. Baykov, A. M. Malinen, H. H. Luoto, R. Lahti, *Microbiol. Mol. Biol. Rev.* **2013**, *77*, 267–276.
- [3] M. Baltscheffsky, A. Schultz, H. Baltscheffsky, *FEBS Lett.* **1999**, *452*, 121–127.
- [4] R. Docampo, W. de Souza, K. Miranda, P. Rohloff, S. N. J. Moreno, *Nat. Rev. Microbiol.* **2005**, *3*, 251–261.
- [5] M. Maeshima, *Eur. J. Biochem.* **1991**, *196*, 11–17.
- [6] N. Mitsuda, K. Enami, M. Nakata, K. Takeyasu, M. H. Sato, *FEBS Lett.* **2001**, *488*, 29–33.
- [7] J. Paez-Valencia, A. Patron-Soberano, A. Rodriguez-Leviz, J. Sanchez-Lares, C. Sanchez-Gomez, P. Valencia-Mayoral, G. Diaz-Rosas, R. Gaxiola, *Plant Sci.* **2011**, *181*, 23–30.
- [8] D. G. Robinson, M. Hoppenrath, K. Oberbeck, P. Luykx, R. Ratajczak, *Bot. Acta* **1998**, *111*, 108–122.
- [9] R. Docampo, V. Jimenez, S. King-Keller, Z.-H. Li, S. N. J. Moreno, in *Adv. Parasitol.*, NIH Public Access, **2011**, pp. 307–324.
- [10] M. T. McIntosh, Y. M. Drozdowicz, K. Laroia, P. A. Rea, A. B. Vaidya, *Mol. Biochem. Parasitol.* **2001**, *114*, 183–195.
- [11] N. R. Shah, K. Vidilaseris, H. Xhaard, A. Goldman, *AIMS Biophys.* **2016**, *3*, 171–194.
- [12] R. Docampo, S. N. J. Moreno, *Curr. Pharm. Des.* **2008**, *14*, 882–888.
- [13] M. Zhang, C. Wang, T. D. Otto, J. Oberstaller, X. Liao, S. R. Adapa, K. Udenze, I. F. Bronner, D. Casandra, M. Mayho, J. Brown, S. Li, J. Swanson, J. C. Rayner, R. H. Y. Jiang, J. H. Adams, *Science* **2018**, *360*, eaap7847.
- [14] G. Lemercier, S. Dutoya, S. Luo, F. A. Ruiz, C. O. Rodrigues, T. Baltz, R. Docampo, N. Bakalara, *J. Biol. Chem.* **2002**, *277*, 37369–37376.
- [15] J. Liu, D. Pace, Z. Dou, T. P. King, D. Guidot, Z. H. Li, V. B. Carruthers, S. N. J. Moreno, *Mol. Microbiol.* **2014**, *93*, 698–712.
- [16] C. O. Rodrigues, D. A. Scott, B. N. Bailey, W. De Souza, M. Benchimol, B. Moreno, J. A. Urbina, E. Oldfield, S. N. J. Moreno, *Biochem. J.* **2000**, *349*, 737–745.
- [17] K. M. Li, C. Wilkinson, J. Kellosalo, J. Y. Tsai, T. Kajander, L. J. C. Jeuken, Y. J. Sun, A. Goldman, *Nat. Commun.* **2016**, *7*, 13596.
- [18] S. M. Lin, J. Y. Tsai, C. D. Hsiao, Y. T. Huang, C. L. Chiu, M. H. Liu, J. Y. Tung, T. H. Liu, R. L. Pan, Y. J. Sun, *Nature* **2012**, *484*, 399–403.
- [19] J. Kellosalo, T. Kajander, K. Kogan, K. Pokharel, A. Goldman, *Science* **2012**, *337*, 473–476.
- [20] K. Vidilaseris, A. Kiriazis, A. Turku, A. Khattab, N. G. Johansson, T. O. Leino, P. S. Kiuru, G. Boije af Gennäs, S. Meri, J. Yli-Kauhaluoma, H. Xhaard, A. Goldman, *Sci. Adv.* **2019**, *5*, eaav7574.
- [21] Y. Zhang, A. Borrel, L. Ghemtio, L. Regad, G. Boije af Gennäs, A. C. Camproux, J. Yli-Kauhaluoma, H. Xhaard, *J. Chem. Inf. Model.* **2017**, *57*, 499–516.
- [22] K. Vidilaseris, J. Kellosalo, A. Goldman, *Anal. Methods* **2018**, *10*, 646–651.
- [23] K. Vidilaseris, N. G. Johansson, A. Turku, A. Kiriazis, G. Boije af Gennäs, J. Yli-Kauhaluoma, H. Xhaard, A. Goldman, *J. Vis. Exp.* **2019**, (153), e60619.
- [24] N. G. Johansson, A. Turku, K. Vidilaseris, L. Dreano, A. Khattab, D. Ayuso Pérez, A. Wilkinson, Y. Zhang, M. Tamminen, E. Grahzdankin, A. Kiriazis, C. W. G. Fishwick, S. Meri, J. Yli-Kauhaluoma, A. Goldman, G. Boije af Gennäs, H. Xhaard, *ACS Med. Chem. Lett.* **2020**, *11*, 605–610.
- [25] S. Cherukupalli, R. Karpoornath, B. Chandrasekaran, G. A. Hampannavar, N. Thapliyal, V. N. Palakollu, *Eur. J. Med. Chem.* **2017**, *126*, 298–352.
- [26] S. D. M. Candice, T. S. Feng, R. Van Der Westhuyzen, R. K. Gessner, L. J. Street, G. L. Morgans, D. F. Warner, A. Moosa, K. Naran, N. Lawrence, H. I. M. Boshoff, C. E. Barry, C. J. Harris, R. Gordon, K. Chibale, *Bioorg. Med. Chem.* **2015**, *23*, 7240–7250.
- [27] K. Figarella, S. Marsiccobetre, I. Galindo-Castro, N. Urdaneta, J. C. Herrera, N. Canudas, E. Galarraga, *Curr. Bioact. Compd.* **2018**, *14*, 234–239.
- [28] L. F. S. P. Azeredo, J. P. Coutinho, V. A. P. Jabor, P. R. Feliciano, M. C. Nonato, C. R. Kaiser, C. M. S. Menezes, A. S. O. Hammes, E. R. Caffarena, L. V. B. Hoelz, N. B. de Souza, G. A. N. Pereira, I. P. Cerávolo, A. U. Krettli, N. Boechat, *Eur. J. Med. Chem.* **2017**, *126*, 72–83.
- [29] Y. Tian, D. Du, D. Rai, L. Wang, H. Liu, P. Zhan, E. De Clercq, C. Pannecouque, X. Liu, *Bioorg. Med. Chem.* **2014**, *22*, 2052–2059.
- [30] M. R. Berthold, N. Cebron, F. Dill, T. R. Gabriel, T. Kötter, T. Meinl, P. Ohl, C. Sieb, K. Thiel, B. Wiswedel, in *Data Anal. Mach. Learn. Appl.*, Springer, Berlin, Heidelberg, **2008**, pp. 319–326.
- [31] J. J. Irwin, T. Sterling, M. M. Mysinger, E. S. Bolstad, R. G. Coleman, *J. Chem. Inf. Model.* **2012**, *52*, 1757–1768.
- [32] E. S. Childress, J. M. Wieting, A. S. Felts, M. M. Breiner, M. F. Long, V. B. Luscombe, A. L. Rodriguez, H. P. Cho, A. L. Blobaum, C. M. Niswender, K. A. Emmitte, P. J. Conn, C. W. Lindsley, *J. Med. Chem.* **2019**, *62*, 378–384.
- [33] M. Pagano, C. Faggio, *Cell Biochem. Funct.* **2015**, *33*, 351–355.
- [34] M. T. McIntosh, A. B. Vaidya, *Int. J. Parasitol.* **2002**, *32*, 1–14.
- [35] Schrödinger: Small-Molecule Drug Discovery Suite **2019–4**. Schrödinger, LLC: New York **2019**.
- [36] BIOVIA: Dassault Systèmes. Discovery Studio **2019**; Dassault Systèmes: San Diego, CA, USA, **2019**.
- [37] W. Trager, J. B. Jensen, *Science* **1976**, *193*, 673–675.
- [38] H. C. Hoppe, J. A. Verschoor, A. I. Louw, *Exp. Parasitol.* **1991**, *72*, 464–467.
- [39] M. Smilkstein, N. Sriwilajaroen, J. X. Kelly, P. Wilairat, M. Riscoe, *Antimicrob. Agents Chemother.* **2004**, *48*, 1803–1806.

Manuscript received: June 1, 2021

Revised manuscript received: August 3, 2021

Accepted manuscript online: August 30, 2021

Version of record online: October 12, 2021